THE JOURNAL OF PHYSICAL CHEMISTRY B

Article

pubs.acs.org/JPCB

Relation Between the Diffusivity, Viscosity, and Ionic Radius of LiCl in Water, Methanol, and Ethylene Glycol: A Molecular Dynamics Simulation

Parveen Kumar,[†] Srinivasa R. Varanasi,[†] and S. Yashonath*[,†,‡]

[†]Solid State and Structural Chemistry Unit, and [‡]Center for Condensed Matter Theory, Indian Institute of Science, Bangalore 560012 India

ABSTRACT: A molecular dynamics (MD) investigation of LiCl in water, methanol, and ethylene glycol (EG) at 298 K is reported. Several structural and dynamical properties of the ions as well as the solvent such as self-diffusivity, radial distribution functions, void and neck distributions, velocity autocorrelation functions, and mean residence times of solvent in the first solvation shell have been computed. The results show that the reciprocal relationship between the self-diffusivity of the ions and the viscosity is valid in almost all solvents with the exception of water. From an analysis of radial distribution functions and coordination numbers the nature of hydrogen bonding within the solvent and its influence on the void and neck distribution becomes evident. It is seen that the solvent−solvent interaction is important in EG while solute−solvent interactions dominate in water and methanol. From Voronoi tessellation, it is seen that the voids and necks within methanol are larger as compared to those within water or EG. On the basis of the void and neck distributions obtained from MD simulations and literature experimental data of limiting ion conductivity for various ions of different sizes, we show that there is a relation between the void and neck radius on the one hand and dependence of conductivity on the ionic radius on the other. It is shown that the presence of large diameter voids and necks in methanol is responsible for maximum in limiting ion conductivity (λ^0) of TMA^+, while in water and EG, the maximum is seen for Rb^+. In the case of monovalent anions, maximum in λ^0 as a function ionic radius is seen for Br^- in water and EG but for the larger ClO_4^- ion in methanol. The relation between the void and neck distribution and the variation in λ^0 with ionic radius arises via the Levitation effect which is discussed. These studies show the importance of the solvent structure and the associated void structure.

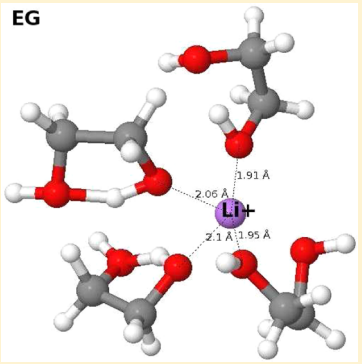

1. INTRODUCTION

The characterization of the structural and dynamical aspects of the solvation of the ion is important due to its role in various chemical and biological processes.[1−3] In recent years, there has been considerable attention[3−9] paid to the effect of ions on the solvent structure, solvation dynamics (i.e., reorientation of solvent molecules in the vicinity of ions), etc. These have led to a better understanding at the microscopic level, but certain issues such as the extent of perturbation caused by the ion on the solvent structure, the structure-maker/structure-breaker role of the ion, transition from structure maker to structure breaker, etc. are still widely debated in the literature. Also, it is not clear how the variation in solvent density and the structural arrangements of solvent molecules influences the ion−solvent interaction and its overall impact on the size-dependence of ionic conductivity.

Studies with experimental techniques such as X-ray and neutron diffraction, X-ray absorption spectroscopy, etc. can only provide equilibrium or average distribution of the solvation shells around the ion and its dynamics.[3,10] Computer simulation techniques can provide a better description of both the structure and dynamics of the ion solvation at the microscopic level and thus provide a more comprehensive picture. In the literature, several simulation studies have been reported using either optimized empirical potentials or quantum mechanical (QM) methods.[10−12] In QM based approaches due to computational limitations, only a few solvent molecules can be included to explore the ion−solvent interaction or solvation structure. Often the observed behavior may be different from what is seen in the many solvent molecules explored through optimized empirical potentials. It is of interest to compare the ion solvation and its dynamics in solvents with different densities and geometrical structures. Such a study may shed some light at the microscopic level on underlying causes for the breakdown of the Stokes−Einstein−Walden framework[13−15] which is a macroscopic approach to interpreting the experimental observations of ionic conductivity as a function of ionic radii in various polar solvents.

There have been several studies investigating the relationship between the limiting ion conducitivity or self-diffusivity of the solute in a solvent and its relationship to the viscosity of the solution. In a molecular dynamics investigation, van Gunsteren and co-workers[16] showed that the product of viscosity (η) and self-diffusion coefficient (D) of pure water is dependent on the

Received: April 15, 2013
Revised: June 18, 2013
Published: June 26, 2013

mass of water, suggesting a deviation from Stokes' law. The inverse relationship between self-diffusivity and viscosity has been found to be valid through the range of density for a hard sphere fluid studied by Alder et al.[17] The relationship between D and η has been shown to be valid over 5 orders of magnitude by Berner and Kivelson.[18] The dependence of D on η in protein solutions has been studied by Lamanna et al.[19] They verified the validity of the Stokes−Einstein relationship as a function of concentration. There have been a number of studies attempting to understand the $D-\eta$ relationship in supercooled liquids but these will not be discussed here. The Stokes−Einstein (SE) relation

$$D = \frac{RT}{N_A 6\pi\eta r_i} \tag{1}$$

which is normally valid for neutral solutes has been found to be not applicable to ions. Any deviations in self-diffusivity from the SE relation can be attributed to either the viscosity or the ionic radius. There have been several reports in the literature where the enhanced diffusivity over and above the Stokes−Einstein value of even neutral solutes has been attributed to the viscosity by the use of a fractional exponent (usually $\eta^{2/3}$) instead of the solute diameter in the Stokes−Einstein expression (the work by Willeke[20] and the papers therein).

In this paper, we report a comparative study of the solvation structure and dynamics of the ions (viz., Li^+ and Cl^-) and solvent molecules using molecular dynamics simulations of LiCl in water, methanol, and EG at 298 K. The relation between the self-diffusivity and solvent viscosity in these and other solvents are investigated. We compare the radial distribution functions like Li^+-O, Cl^--O, and O−O and the average co-ordination number of Li^+, Cl^-, and solvent molecules obtained from the MD simulation of LiCl in water and methanol with the reported experimental and simulation results. The distribution of void and bottleneck radius present within these liquids are then obtained through Voronoi tessellation. These are then used to understand the experimental data on the limiting ion conductivity of ions of different sizes within these three solvents.

2. METHODS

2.1. Intermolecular Potentials and Models. The SPC/E model for water has been used in the present study.[21] In this model, water is represented by three interaction sites positioned on O and H atoms. The O−H bond length is taken to be 1.0 Å, and the HOH angle is equal to the tetrahedral angle 109.47°. A charge of +q is placed on H and −2q on O. The short-range Lennard-Jones interaction exists only for oxygen. For methanol, we have used a Haughney's-(H1) rigid three site model,[22,23] in which the methyl group is represented by a single site within the united atom model, the second site by oxygen, and the third by hydrogen, where all sites act as both Lennard-Jones and charge interaction sites. In these models, the potential of interaction between the various sites located either on the solvent or the ion is of the form

$$\Phi(r_i, r_j) = 4\varepsilon_{ij}\left[\left(\frac{\sigma_{ij}}{r_{ij}}\right)^{12} - \left(\frac{\sigma_{ij}}{r_{ij}}\right)^{6}\right] + \sum_{i,j,i\neq j}\frac{q_i q_j}{r_{ij}} \tag{2}$$

where ε_{ij} is the well depth, σ_{ij} is the Lennard-Jones diameter, and r_{ij} is the distance between atomic sites or ions. q_i and q_j are the charges at sites i and j, respectively. The cross interaction terms of Lennard-Jones parameters have been calculated by using the standard Lorentz−Berthelot mixing rules (i.e., $\sigma_{ij} = {}^1/_2(\sigma_i + \sigma_j)$ and $\varepsilon_{ij} = (\varepsilon_{ii}\varepsilon_{jj})^{1/2}$). Ions Li^+ and Cl^- have been modeled as single sites with charge.[24,25] All of the interaction potential parameters used in this study are listed in Table 1.

Table 1. Self-Interaction Parameters for the Two Solvents, Water and Methanol, As Well As the Li^+ and Cl^- Ions

solvent/ion	atom/group	σ (Å)	ε (kJ/mol)	charge (q)
water(spc/e)	O	3.169	0.6502	−0.8476
	H	0.000	0.000	+0.4238
CH_3OH	CH_3	3.861	0.7576	0.297
	O	3.083	0.7309	−0.728
	H	0.000	0.000	0.431
Li^+	Li	1.5050	0.6904	+1
Cl^-	Cl	4.4010	0.4184	−1

Ethylene Glycol (EG). The initial conformation has been chosen to be the most stable conformer (i.e., g'Gt) of EG.[26] We have used all atom OPLS force field (OPLS-AA) for EG. This was originally developed by Jorgensen and co-workers[27] and recently optimized by Szefczyk and Cordeiro.[28] This model allows for variation in bond length, bond angle, and dihedral angle. Parameters for the bond stretching and bond angle variation have been taken from Jorgensen and co-workers.[27] All parameters for the torsional potential have been used from Jorgensen et al.[27] with the exception of the C−C−O−H and O−C−C−O which have been taken from Szefczyk and Cordeiro.[28]

This is because use of just three dihedral angles for EG within the Szefczyk and Cordeiro's model led to instability in MD integrations in the presence of ions. Further, we note that none of the intermolecular potential functions have been tested for the MD simulation of ions in EG. Density is one of the important factor in determining the void-neck distribution in solvents. The optimized AA model of EG by Szefczyk and Cordeiro reproduces the experimental density whereas majority of the other models underestimates the density. Also, the diffusivity of the pure EG reported by Szefczyk and Cordeiro is closer to the experimental value. See Table 4 of Szefczyk and Cordeiro.[28]

For the nonbonding interaction separated by three bonds (i.e., 1−4 interaction), we have used the standard scaling factor of 0.5 for both Coulomb and Lennard-Jones interactions.[27,28] For Li^+ and Cl^- ions in EG, we have used the OPLS parameters from Fennel et al.[29] in which cross terms of Lennard-Jones parameters are calculated by taking geometric means for both σ_{ij} and ε_{ij} (i.e., $\sigma_{ij} = (\sigma_{ii}\sigma_{jj})^{1/2}$ and $\varepsilon_{ij} = (\varepsilon_{ii}\varepsilon_{jj})^{1/2}$). All of the Lennard-Jones potential parameters for EG, Li^+ and Cl^- ions are listed in Table 2.

Table 2. OPLS-AA Nonbonded Parameters for Ethylene Glycol (EG) and OPLS Parameters for Li^+ and Cl^- Ion

solvent/ion	atom/group	σ (Å)	ε (kcal/mol)	charge (q)
EG	C	3.50	0.066	0.165
	H	2.50	0.030	0.060
	O	3.00	0.170	−0.720
	Ho	0.00	0.000	0.435
Li^+	Li	2.1264	0.01828	+1
Cl^-	Cl	4.4172	0.11779	−1

dx.doi.org/10.1021/jp4036919 | J. Phys. Chem. B 2013, 117, 8196−8208

Table 3. Diffusion Coefficient (D) and Limiting Ion Conductivity (λ^0)[44−46] of Li^+ and Cl^- Ions in Water, Methanol, and EG in Addition to Some Properties of the Pure Solvents

ion	λ^0 (S cm^2 mol^{-1})	10^9 D (m^2 s^{-1})	solvent	ρ (g cm^{-3})	η (mPa s)	μ (D)	ε
Li^+ (methanol)	39.55	0.65	methanol	0.7865[47]	0.545[47]	1.70[48]	32.6[47]
Li^+ (water)	38.84	1.091	water	0.9970[44]	0.8903[44]	1.85[49]	78.5[50]
Li^+ (EG)	2.10	0.02	EG	1.1095[51]	16.19[51]	2.28[49]	40[49]
Cl^- (methanol)	52.36	0.82					
Cl^- (water)	76.36	1.47					
Cl^- (EG)	5.07	0.03					

2.2. Simulation Details. All simulations were done using molecular dynamics technique and were performed in the NVE ensemble using the DLPOLY program.[30] Simulations were performed on a system consisting of 8 ion pairs (i.e., Li^+ and Cl^-) in 848 solvent molecules in a cubic simulation box. The length of the simulation cells were obtained from the liquid density of the solvents (i.e., water, methanol, and EG) at 298 K and 1 bar pressure (see Table 3). These are 29.5877, 38.8107, and 43.1357 Å for Li^+ and Cl^- ions in water, methanol, and EG, respectively. These have been used in the MD simulations. Periodic boundary conditions were applied in all three directions. The velocity Verlet algorithm has been used to solve the Newton's equations of motion. Long range forces were computed with the help of the Ewald sum.[31] For LiCl in water and methanol, a time step of 1 fs was used which gave good conservation of energy. The system was equilibrated for 500 ps during which the velocities were scaled to the desired temperature followed by 2.0 ns production run during which position coordinates and velocities of ions were stored at an interval of 10 fs. In case of LiCl in EG, we have used a time step of 0.5 fs, and the system was equilibrated for 700 ps followed by a 4.0 ns production run during which data were stored every 25 fs. In these calculations, we have employed cutoff radii of 14.0, 19.4, and 17.0 Å for water, methanol, and EG respectively.

2.3. Voronoi Tessellation. We have carried out Voronoi construction to characterize the structure of the "pore space" (also referred to as "void space") in the liquid following the previous work of a similar nature in liquids[32,33] and powders or disordered media.[34,35] This provides the distribution of voids and narrower bottlenecks that connect two or more voids. Such information is valuable in the study of liquids as we have previously shown, especially to understand the Stokes−Einstein relationship.[36] A Voronoi polyhedron defines a subset of volume of all points that are closer to i (where i is the central atom) than to any other particle. All particles are assumed to be spheres. The vertices are equidistant from the closest surrounding particles. So are edges. In disordered systems a vertex is equidistant from four closest particles while a point on the edge is equidistant from three particles. The network of the polyhedron defined by the edges provides a natural and convenient description of the void space. The distance of the vertex to the closest particle minus the particle diameter is the radius of the void. The radii of the channels (referred to as bottlenecks or simply "necks") interconnecting voids are given by the distance of an edge to the closest particle minus the radius of the particle. These are illustrated in two dimensions with the help of the Figure 1. Diffusants of a given radius can find an interconnected path between voids if the intervening neck sizes are larger than the diffusant radius. However, the motion of the solvent atoms ensure that the void network is restructured dynamically. Thus, even for an ion for which there is no interconnected path at a given time step manages to diffuse over a period of time. Voronoi and Delaunay tesselations have been carried out using the algorithm by Tanemura, Ogawa, and Ogita,[37] as outlined in Sastry et al.[33] For each molecular dynamics run, the void and neck sizes are calculated from ten configurations and binned with $\Delta r_v = \Delta r_n = 0.01$ Å using the positions of the solvent particles. We note that although there are previous attempts to represent a molecule by more than one sphere and thereby take into account the geometry of the molecule, it is not clear if these methods yield any better insight into void and neck distribution.[38−40] We have therefore used single spherical site for each of the molecule of solvent. We have computed the diameters for water and methanol molecules from their van der Waals volume. For EG, we have used kinetic diameter from the literature. The diameters are 2.87, 3.46, and 4.50 Å for the three solvents water, methanol and EG respectively. These values are consistent with kinetic diameters of these solvent molecules suggested by different groups.[41−43]

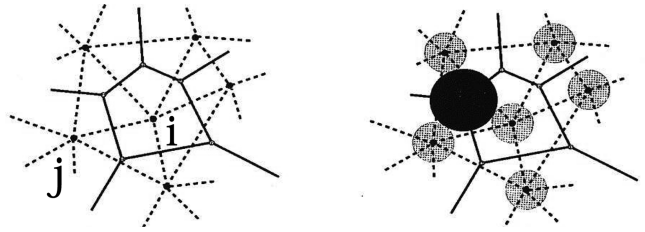

Figure 1. Two-dimensional illustration of the Voronoi−Delaunay dual construction. The central atom i is surrounded by atoms (termed j). The figure has been taken from Corti et al.[32]

3. RESULTS AND DISCUSSIONS

3.1. Diffusion of Ions in Water, Methanol, and EG. Figure 2a,b shows the mean square displacement (MSD) of Li^+ and Cl^- ions in water and methanol at 298 K. The slope for both ions is higher in water as compared to that in methanol. In Figure 2c, we show the MSD plot for Li^+ and Cl^- in EG at 298 K. The slopes for Li^+ and Cl^- in EG are significantly lower as compared to those for water and methanol. The diffusivities of the ions have been calculated from the slope of the MSD using Einstein's equation:[31]

$$D = \frac{\langle u^2(t)\rangle}{2dt} \tag{3}$$

where $\langle u^2(t)\rangle$ is the average mean squared displacement over time t and d (taken to be 3) is the dimensionality. In Table 3, we list the self-diffusion coefficient (D) obtained from MD simulation for Li^+ and Cl^- ion in water, methanol, and EG along with the limiting ion conductivities(λ°) of these ions from the literature.[44−46] The conductivity and diffusivity are related through the Nernst−Einstein equation:

dx.doi.org/10.1021/jp4036919 | J. Phys. Chem. B 2013, 117, 8196−8208

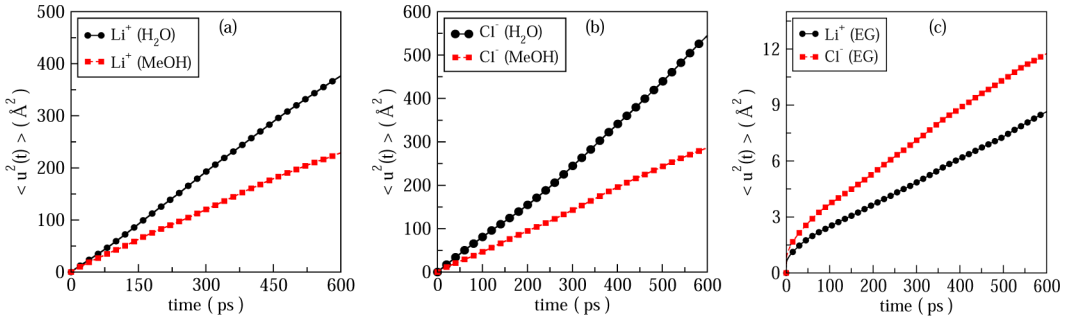

Figure 2. Mean square displacement of Li^+ and Cl^-ion in water, methanol, and EG at 298 K.

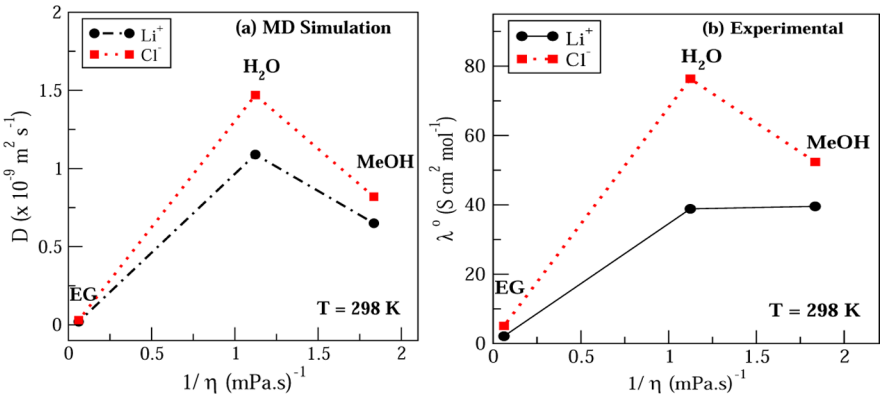

Figure 3. (a) Plot shows the variation of self-diffusion coefficient (D) as a function of solvent viscosity for Li^+ and Cl^- ion in water (H_2O), methanol (MeOH), and EG at 298 K. (b) Plot of limiting ion conductivity (λ^0) versus viscosity of the solvents for the Li^+ and Cl^- ion at 298 K. The λ^0 values of Li^+ and Cl^- ions in water, methanol, and EG are taken from the literature.[44−46]

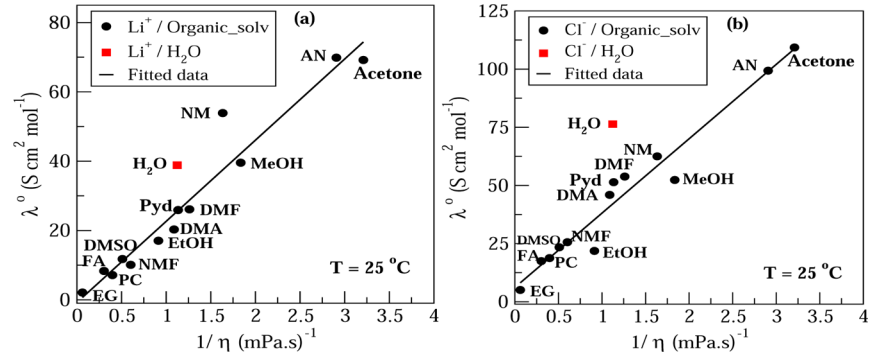

Figure 4. Plot of limiting ion conductivity (λ^0) versus viscosity for (a) Li^+ and (b) and Cl^- ion in different solvents at 25 °C. The viscosity data of acetone, acetonitrile (AN), methanol (MeOH), nitromethane (NM), dimethylformamide (DMF), pyridine (Pyd), dimethylacetamide (DMA), ethanol (EtOH), *N*-methylformamide (NMF), dimethylsulfoxide (DMSO), propylene carbonate (PC), and formamide (FA) are taken from Krumgalz[55] whereas for water(H_2O) and ethylene glycol (EG) from Ueno et al.[44] and Sieno et al.,[51] respectively. All λ^0 values of Li^+ and Cl^- in the above solvents except in water, acetonitrile, methanol, and EG are taken from the Krumgalz.[55] The λ^0 values of Li^+ and Cl^- ion in water, acetonitrile, methanol, and EG are taken from Ueno et al.,[44] Safonova et al.,[56] Kay and Evans,[45] and Kalugin et al.,[46] respectively.

$$\lambda = \frac{N_{ion} e^2 D}{V k_B T} \tag{4}$$

where N_{ion} is the number of ions in a simulation cell of volume V and e is the electronic charge. T is the temperature of the calculation. Limiting ion conductivity is conductivity of the solution in the limit of infinite dilution.

The experimental limiting ion conductivities λ^0, self-diffusivities from MD, viscosities, densities, dipole moments, and dielectric constants for the three solvents studied here are listed in Table 3. In order to understand the variation of the diffusivity for a given solute in different solvents, we have plotted diffusivity against reciprocal viscosity in Figure 3a for the three solvents. From Walden's rule we know that the product of limiting ion conductivity or self-diffusivity and viscosity should be constant ($\lambda^0\eta_0$ = constant).[52] It is well-known that the Walden product is not constant when plotted as a function of ionic radius leading to an anomalous maximum in Walden product for ions of certain sizes.[13,14,53,54] However, many previous studies have suggested that the reciprocal relation between limiting ion conductivity or diffusivity and viscosity is valid.[17] These were earlier discussed in the introduction. There are also reports where the deviation from reciprocal dependence between self-diffusivity of the solute and

dx.doi.org/10.1021/jp4036919 | J. Phys. Chem. B 2013, 117, 8196−8208

viscosity were attributed to $D \propto \eta^{2/3}$. We see that the three points for Li^+ as well as Cl^- do not fall on a straight line. Thus, the Walden product is not constant for a given ion over this range of viscosities. We have also plotted the limiting ion conductivity λ^0 against reciprocal viscosity in the same figure (see Figure 3b). Note that this also exhibits a similar trend as the MD result. It is not clear from this plot (Figure 3) which of the three points really is deviating from the expected reciprocal dependence between λ^0 or diffusivity and viscosity. In order to understand this better, we plotted the limiting ion conductivity data for Li^+ as well as Cl^- ions including data from several more solvents. This is shown in Figure 4. From this plot it is evident that the reciprocal dependence between λ^0 and η is indeed valid over a wide range of solvents with the exception of water and probably nitromethane (for Li^+ ion). For water and possibly nitromethane, the limiting ion conductivities of Li^+ (and Cl^-) are higher than can be obtained from the SE expression. The origin of this higher diffusivity could lie in the anomalous dependence of diffusivity on ionic radius discussed later.

As shown in the Table 3, the self-diffusion coefficient of Li^+ and Cl^- ions is highest in water and lowest in EG at 298 K. The limiting ion conductivity (λ^0) value of Cl^- ion is higher in water than methanol and EG which is in agreement with MD results. In case of Li^+, λ^0 value is slightly higher in methanol than water whereas MD results show lower D value in methanol as compared to water. The λ^0 value of Li^+ is lowest in EG which is in agreement with the trend observed in MD results.

The value of self-diffusivity of pure solvents obtained by us from the MD simulation are 2.32×10^{-9} m^2 s^{-1} (actual temperature is 295.3 K) for water, 1.96×10^{-9} m^2 s^{-1} (295.5 K) for methanol, and 0.04×10^{-9} m^2 s^{-1} (299.3 K) for EG. These may be compared with those reported in the literature obtained from simulations: 2.4×10^{-9} m^2 s^{-1}, 2.8×10^{-9} m^2 s^{-1}, etc. for SPC/E water model,[57,58] 1.8×10^{-9} m^2 s^{-1} and 2.6×10^{-9} m^2 s^{-1} for methanol,[23,59] and 0.025×10^{-9} m^2 s^{-1}, 0.17×10^{-9} m^2 s^{-1}, 0.74×10^{-9} m^2 s^{-1}, and 0.15×10^{-9} m^2 s^{-1} for EG.[28,60] The reported experimental D values are 2.3×10^{-9} m^2 s^{-1}, 2.4×10^{-9} m^2 s^{-1}, and 0.09×10^{-9} m^2 s^{-1} for water,[61] methanol,[62] and EG,[63] respectively, at 298 K.

Velocity autocorrelation functions (VACF) for the Li^+ ion in methanol, water, and EG show more pronounced oscillations (see Figure 5a). This suggests that the ion is well caged by the solvent molecules leading to significant oscillations. Oscillations seen in water and methanol are similar in nature which is consistent with similar values for the conductivity of lithium ions in these solvents. In EG it is seen that the oscillations decay slowly extending up to 0.6 ps as compared to in water or methanol where the oscillations decay by about 0.3 ps. For the Cl^- ion, it is seen that the amplitudes of oscillations are largest for EG and least for water, and the self-diffusivities of the chloride ion in these solvents are at a maximum in water and a minimum in EG.

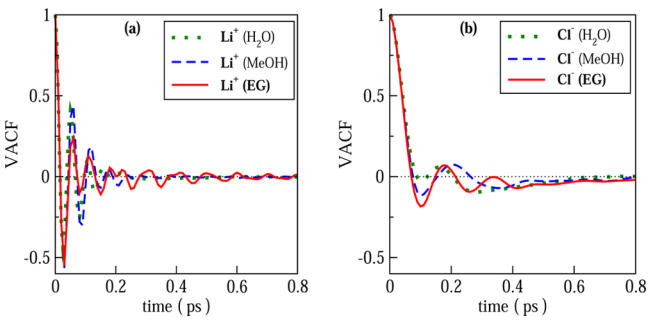

Figure 5. Velocity autocorrelation functions for Li^+ and Cl^- ion in water, methanol, and EG at 298 K.

3.2. Solvation Structure. In order to understand the structure within the liquids and around the ions, we have computed the three radial distribution functions (RDFs) (i.e., O−O, Li^+−O, and Cl^-−O) along with the coordination number for solute as well as solvent. The running coordination number is obtained by integrating the respective RDFs, $g(r)$

$$n(r) = 4\pi\rho \int_0^r r'^2 g(r')\, dr' \tag{5}$$

where ρ is the number density and r' is the separation between the two species. Figure 6a,b shows the O−O RDF for water and methanol, respectively. Note that in EG, O−O RDF does not include the intramolecular O−O, but only intermolecular O−O is included. A first peak is seen around 2.8 Å in both solvents, but the first coordination numbers are different: 5.0 for water and 2.4 for methanol. This indicates a high degree of association at short-range in water as compared to methanol. The first minima in O−O RDF appears at ~3.5 Å in methanol and at 3.4 Å in water. Also, a less intense second peak is seen at an average distance of 4.5 Å in water and at 4.88 Å in methanol. The peak positions in O−O RDF of water and methanol are in close agreement with the values reported in the literature.[64−68] The coordination number from O−O RDF for water is 5.0, suggesting a near tetrahedral arrangement between hydrogen-bonded water molecules with may be one extra non-hydrogen bonded water molecule in the first solvation shell (FSS). For methanol, the coordination number from O−O RDF is 2.4, indicating that each molecule tends to form only two H-bonds leading to a linear chain[23,69] or alternately cyclic clusters.[70] The estimate of coordination number obtained here is in good agreement with the values reported in the literature, which varies between 4.4 and 5.2[64,65,71] for water and 1.87 and 2.2 for methanol.[23,66−68] In the case of EG, as shown in Figure 6c, a first peak in O−O RDF appears at 2.6 Å with a peak height of 2.2, whereas a second peak at 4.7 Å with a peak height of 1.8 which is somewhat different from the value reported by Szefczyk and Cordeiro.[28] These differences arise from the difference in the intermolecular potential used by us here and that used by Szefczyk and Cordeiro.[28]

Figure 7a shows the Li^+−O RDF in water and methanol at 298 K. As shown in Figure 7a, the first peak in Li^+−O RDF appears at ~2.0 Å in both the solvents. Note that the first and second peaks are in the region with zero value for the RDF which suggests no exchange between the FSS and second solvation shell. In case of water, the compilation of Spangberg et al.[72] of the literature values show that, the first peak in Li^+−O RDF appears between 1.95 and 2.20 Å from simulation and 1.94 and 2.07 Å from experimental measurements whereas the average coordination number for Li^+ ion in water varies between 3.7 and 6.1 from simulation and 4.5 and 5.5 from experimental studies. For the Li^+ ion in methanol, the simulation result from Impey et al.[73] shows the first peak at 1.90 Å, Pagliai et al.[74] at 2.0 Å and the peak from the experimental meausrements[75] is reported at 2.06 Å, also the average coordination number reported in the literature for Li^+ in methanol is 4−4.02.[25,73,74] Our results obtained here are in good agreement with these values for both water and methanol. Figure 7b shows the Li^+−O RDF in EG where first peak appears at 2.03 Å with peak height 17.8 and the first minima in

dx.doi.org/10.1021/jp4036919 | J. Phys. Chem. B 2013, 117, 8196−8208

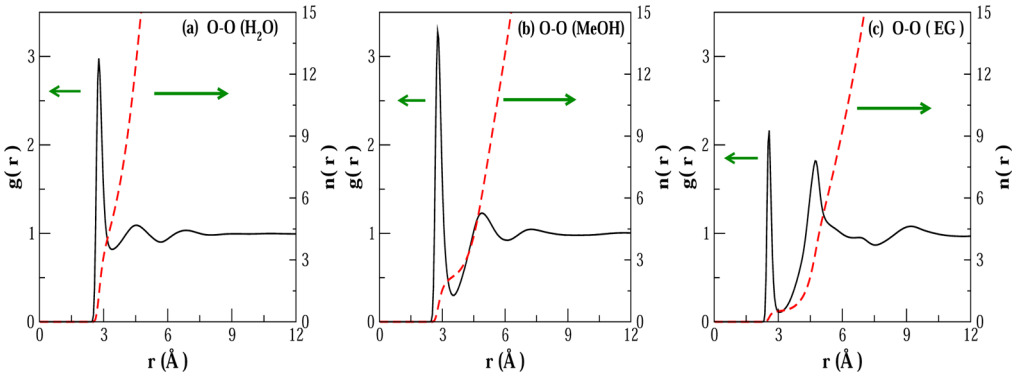

Figure 6. Oxygen−oxygen (O−O) radial distribution function for water, methanol, and EG at 298 K.

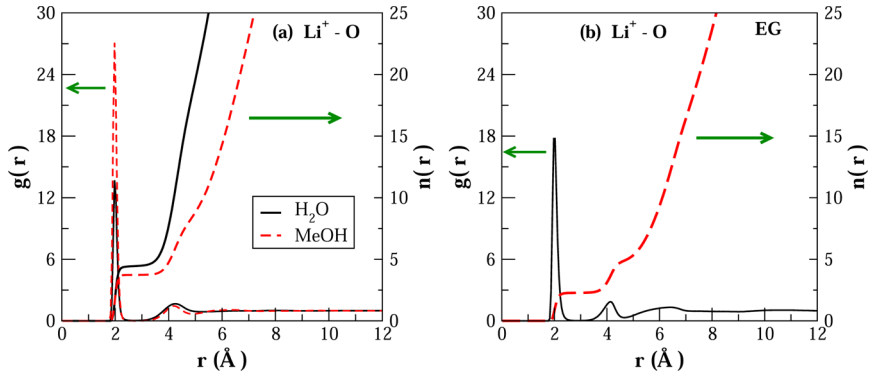

Figure 7. Solute−solvent radial distribution function of Li^+ ion in water, methanol, and EG at 298 K.

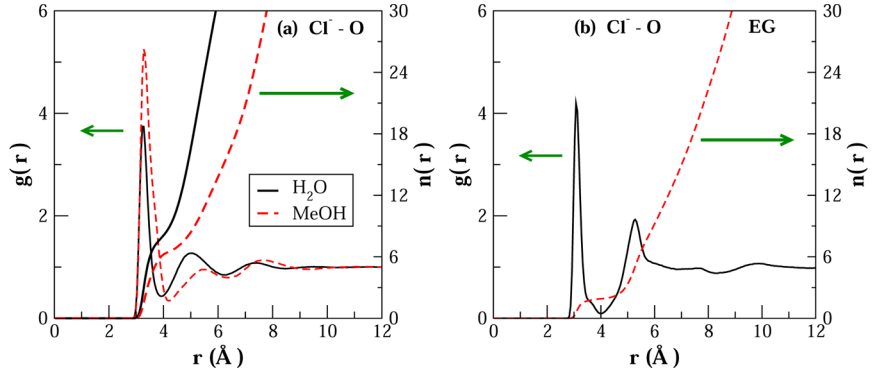

Figure 8. Solute−solvent radial distribution function of the Cl^- ion in water, methanol, and EG at 298 K.

RDF at 3.1 Å . The average coordination number at the first peak of Li^+−O RDF is 2.3.

For Cl^-−O RDF (see Figure 8a), the first peak appears at ∼3.2 Å in both solvents. As shown in Figure 8a, the behavior of running coordination number plot for Cl^-−O RDF indicates a weakly defined FSS in water as compared that in to methanol; the average coordination number is 7.8 in water and 6.5 in presence of methanol. In the literature, the average coordination number reported for Cl^- in water are 7.2−8.36 from MD simulations,[76−79] 5−11 from X-ray experiments,[80] and 5.3−6.2 from neutron diffraction experiments,[81] whereas for the Cl^- ion in methanol the average coordination number reported is 3.56−6.3 from MD simulation.[25,73,74,82] These indicate that the solvation structure around the ion is similar to that obtained in other simulation studies and experiment. In Figure 8b we have plotted the Cl^-−O RDF in EG which shows a first peak at 3.1 Å with peak height 4.2 and the first minima in RDF appears at 4.03 Å with average coordination number of 1.9 for Cl^- ion.

The comparative analysis of Li^+-O RDF in water, methanol and EG shows that the first peak appears at 2.0 Å in all three solvents, but the peak height decreases in the order methanol (27.0) > EG (17.8) > water (13.6). Similarly, the Cl^-−O RDF shows a first peak at 3.2 Å in water and methanol and at 3.0 Å in EG but the peak height decreases in the order methanol (5.2) > EG (4.2) > water (3.7). The above comparison suggests the existence of more structured solvation shell, in comparison to the bulk density of the respective solvent, for the ions in methanol than water and EG. However, we observed from the MSD that the self-diffusion coefficient of ions is very low in EG as compared that in to methanol and water. In this section, we got an idea of the equilibrium structure of the solvent around the ions. In the next section, we will explore the dynamics of

dx.doi.org/10.1021/jp4036919 | J. Phys. Chem. B 2013, 117, 8196−8208

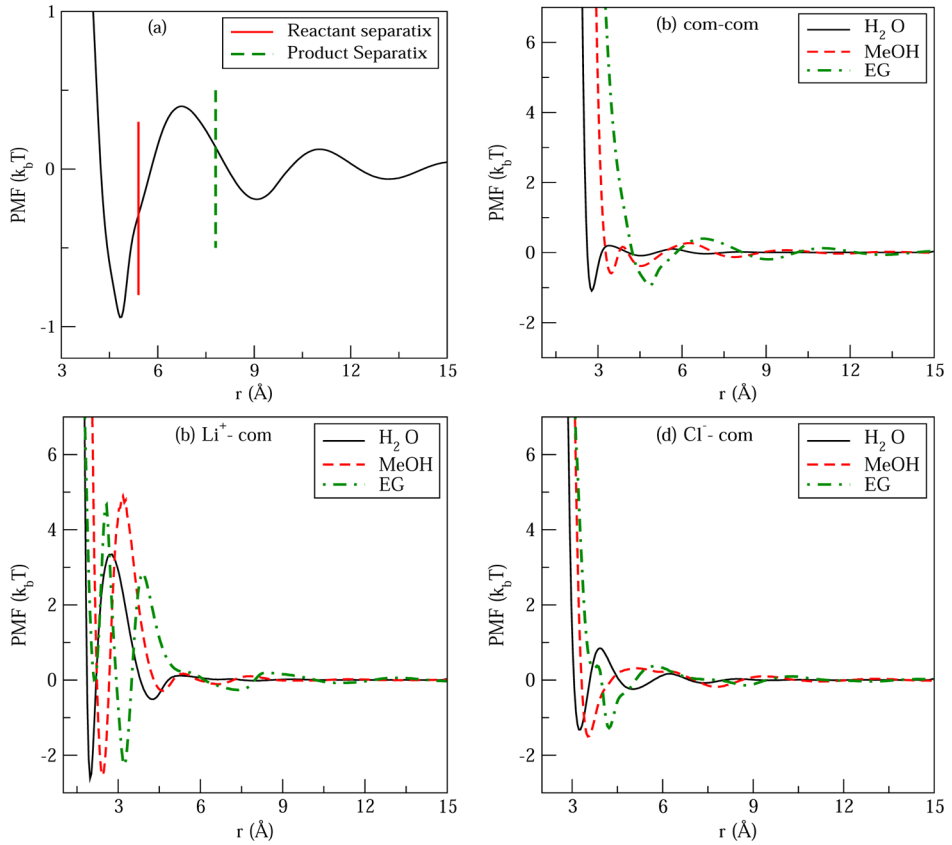

Figure 9. (a) Stable reactant separatix which is the distance at which the PMF is half of the difference between the maximum and minimum (by vertical line) along with the product separatrix (indicated by dashed vertical line) defined similarly. PMF plot for (a) com−com, (b) Li^+−com, and (c) Cl^-−com for water, methanol, and EG at 298 K.

the solvent molecules in the solvation shells of the ions to get better insight into the ion−solvent interactions.

3.3. Mean Residence Time (MRT). In order to understand the influence of the ions, in general, on the solvent molecules and in particular on the exchange of the solvent molecules between the first and the second solvation shells, we have attempted to compute the mean residence times (MRT) of the solvent molecules in the first solvation shell of the solute as well as the solvent. There are at least two well-known approaches available to estimate the MRT such as the suggestion of Impey et al.[83] and the more recent approaches of Laage and Hynes.[84,85] Here we employ the stable states picture (SSP) proposed by the latter. The τ_{SSP}^{res} values are calculated using following relation:

$$1 - \langle P_R(0)P_p(t)\rangle = e^{-t/\tau_{SSP}^{res}} \quad (6)$$

where $P_R(0)$ is the probability of finding the reactant in the stable state at time 0 and $P_p(t)$ is the probability of finding the product in the stable product state at time t. τ_{SSP}^{res} is the mean residence time(MRT). To get the stable reactant and product configuration, we have first calculated the potential of mean force (PMF) $G(r)$ from

$$G(r) = -k_B T \ln g(r) \quad (7)$$

where k_B is the Boltzmann constant, T is the temperature, and $g(r)$ is the pair distribution function of relevant pair (i.e., ion and solvent or solvent and solvent). The reactant separatix and product separatix were obtained as per the prescription of Laage and Hynes (Figure 9).[85] In other words, we have used half the height of the potential well as the cutoff distance for considering the solvent as either in the stable reactant state or product state. The resulting values of MRT are listed in Table 4. In case of EG, we have calculated two MRT values (namely, τ_1 and τ_2) for the two minima in PMF. We have also calculated the MRT of solvent molecules (residence time of one solvent molecule in the FSS of another solvent molecule), which is 7.01 ps for methanol, 4.04 ps for water, and 21.56 ps for EG.

Table 4. Residence Time of com (i.e., Center of Mass) of Water, Methanol, and EG in the FSS of Li^+ and Cl^- at 298 K, Calculated Using the Stable State Picture (SSP) Approach[85]

$g(r)$/solvent	reactant separatix	product separatix	τ_{ssp} (ps)
Li^+−com (methanol)	2.73	3.62	22.19
Li^+−com (water)	2.17	3.39	18.69
Li^+−com (EG)	2.37	2.80	18.64 (τ_1)
	3.53	4.41	18.12 (τ_2)
Cl^-−com (methanol)	3.87	6.83	19.78
Cl^-−com (water)	3.55	4.37	7.56
Cl^-−com (EG)	4.58	6.66	19.08
com−com (methanol)	3.64	4.14	7.01
com−com (water)	2.97	3.91	4.04
com−com (EG)	5.40	7.80	21.56

The mean residence time (MRT) provides insight into the frequency of solvent exchange between the FSS and the second solvent shell of the central species. It is interesting to note that the MRT of methanol and water is significantly high in the FSS

dx.doi.org/10.1021/jp4036919 | J. Phys. Chem. B 2013, 117, 8196−8208

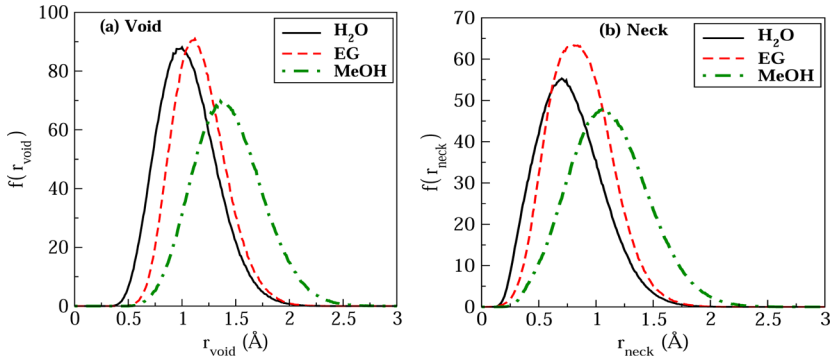

Figure 10. Distribution of void and neck radius in water, methanol, and EG at 298 K.

of ions as compared to FSS of solvent molecules whereas the MRT of EG in FSS of ion and FSS of solvent molecule are comparable. This suggests the dominant role of ion−solvent interaction as compared to the solvent−solvent interaction in the case of water and methanol, whereas in the case of EG, solvent−solvent interactions also play a dominant role. Before we proceed further, it is necessary to understand the structural arrangement of the solvent molecules, hydrogen bonding, and their role in the diffusivity or conductivity of the ions in different solvents.

Another important structural feature of the solution is the void structure of the liquid. Previously, there have been attempts to understand and obtain the size distribution of voids in ionic liquids.[86,87] The calculation of the void and neck distributions[32,33,88]by Sastry et al, Corti et al and others give us an estimate of the sizes of the voids and necks present in dense liquids dominated by van der Waals interaction.

3.4. Void−Neck Distribution in Water, Methanol, and EG. The variation in the solvent density and the geometrical arrangements of the solvent molecules influences the void and neck distribution within solvents. Methanol has the lowest density among the three solvents (see Table 3). Also, at ambient condition, we know that each water molecule forms an H-bond with around 3.5 nearest neighbors, resulting in the formation of three-dimensional fluctuating network structures.[89,90] Such a network of tetrahedral hydrogen-bonded structures leads to a certain distribution of void or cage networks within the water. In the case of methanol, which is a simplest monohydric alcohol, each molecule can form three hydrogen bonds, but on average it is two, giving rise to one-dimensional linear winding chains consisting of these hydrogen bonded molecules.[91,92] EG, a dihydroxy alcohol, is also influenced by the presence of hydrogen bonds. It contains two proton donor hydroxyl groups and two proton acceptor centers, that is, two oxygen atoms. This leads to the existence of a water like three-dimensional hydrogen bond network[93−95] in EG. Also, water and EG have comparable ealsticity of the three-dimensional H-bond network,[96] which is considered as the ability to preserve its initial configuration. However, in contrast to water or monohydroxy alcohols, liquid EG, due to the presence of weakly polar groups (−CH_2−CH_2− group) and polar groups (i.e., −OH groups), exhibits both intermolecular and intramolecular hydrogen-bond interactions. There is, in fact, competition between intermolecular and intramolecular interactions.[97] Tanaka,[98] and also Graziano,[99] have discussed the role of hydrogen bonding in the distrbution of cavities in H-bonded liquids. Their work as well as those of Sanchez and co-workers[100] show that the presence of hydrogen bonding increases the size of the voids in water. This result is probably true for other hydrogen bonded liquids such as methanol and EG as well, although there are no studies in these solvents to date. This has implications for transport properties of ions and other solutes as we shall see below.

While experimental techniques can, at best, provide qualitative evidence about the void-size (and neck-size) distribution in solvents, computer simulation studies can provide direct microscopic information on the structural and dynamical properties of both ions and solvent molecules.[31] Voronoi polyhedral (VP) analysis,[32,33,101] which is used to characterize the structure of the void space in the solvent, is found to yield valuable insights into both the distribution of void and neck radius.

The void and neck distribution in water, methanol and EG were obtained from the Voronoi tessellation of liquid water.[33,37] As shown in Figure 10a, the most probable radius of the void appears at 1.0 Å in water and 1.12 Å in EG, whereas it shifts to 1.36 Å in methanol. Similarly, the most probable radii of the neck in water, EG, and methanol appear at 0.7, 0.79, and 1.05 Å, respectively (see Figure 10b). Normally the void radii within dense liquids and close-packed solids are related to the molecular diameter of the packing sphere, R.[102] Radii of tetrahedral and octahedral voids are respectively 0.225R and 0.414R in face-centered cubic solid. However, as already mentioned above, the presence of hydrogen bonds leads to larger-sized voids as compared to a simple Lennard-Jones liquid.[98,99] In the present case, note that both water and EG are charactersized by a tetrahedral hydrogen bonded network. Surprisingly, although EG has a larger molecular diameter, both water and EG have similar void and neck distribution plots, with the distribution of EG only slightly shifted to larger radius. Methanol which is characterized by two hydrogen bonds per molecule appears to be characterized by much larger voids and necks as compared to both water and EG. This is probably due to its lower density. Further, note that the width of the distribution of void and neck radius are somewhat larger for methanol which also leads to a lower height of the maximum. We shall see below the effect of the void and neck distribution on the properties of diffusion of ions, in particular to the variation of self-diffusivity with ionic radius.[14,53,54]

3.5. Dependence of Conductivity on the Ionic Radius in Water, Methanol, and EG. In the literature, conductivities of many different cations as well as anions have been measured experimentally in the three solvents, water, EG, and methanol. Variation of λ^0 of monovalent ions as a function of ionic radius (r_i) in water, methanol, and EG at 25 °C is shown in Figure 11. All of the data for the plot have been taken from experiments

dx.doi.org/10.1021/jp4036919 | J. Phys. Chem. B 2013, 117, 8196−8208

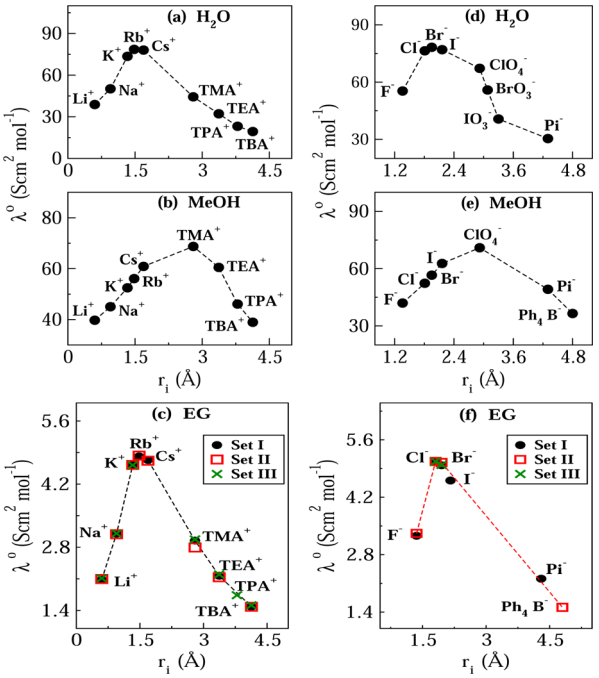

Figure 11. Limiting ionic conductivity (λ^0) of monovalent in water and methanol (MeOH) are plotted as a function of ionic radii (r_i): (a) λ^0 vs r_i for cations in water at 25 °C. The data are taken from Ueno et al. and Nakahara et al.[44,106] (b) λ^0 vs r_i for cations in MeOH at 25 °C. The data are taken from Hefter and Solomon[107]and Kay and Evans.[108] (c) λ^0 for cations at 25 °C from different research groups (i.e., set I: the conductivity data for Li^+, Na^+, K^+, Rb^+, Cs^+, tetramethylammonium (TMA^+), tetraethylammonium (TEA^+), and tetrabutylammonium (TBA^+) ions are from Sieno et al. 1971;[51] set II: λ^0 for Li^+, Na^+, K^+, Rb^+, Cs^+, TMA^+, TEA^+, and TBA^+ are from Kalugin et al. 1998;[46] set III: λ^0 for Li^+, Na^+, K^+, TMA^+, TEA^+, tetrapropylammonium (TPA^+), and TBA^+ are from Santos and Spiro 1972).[109] (d) λ^0 vs r_i for anions (i.e., F^-, Cl^-, Br^-, I^-, perchlorate (ClO_4^-), bromate (BrO_3^-), iodate (IO_3^-), and picrate (Pi^-) ions) in water at 25 °C. The data are taken from Kay and Evans,[108] Broadwater and Kay,[110] and Majeed and Timimi.[111] (e) λ^0 vs r_i for anions in MeOH at 25 °C. The data are taken from Hefter and Solomon,[107] Evers and Knox,[112] and Kunze and Fuoss.[113] (f) λ^0 for anions at 25 °C from different research groups (i.e., set I: the conductivity data for F^-, Cl^-, Br^-, I^-, and Pi^- ions are from Santos and Spiro 1972;[109] set II: λ^0 for F^-, Cl^-, Br^-, I^-, and tetraphenyl borate (Ph_4B^-) ions are from Kalugin et al. 1998;[46] set III: λ^0 for Cl^- and Br^- are from Sieno et al.[51]).

reported in the literature, and citations to original references are provided. In Figure 11a–c, the variation of λ^0 with r_i is shown for monovalent cations in water, methanol, and EG, respectively. The ionic radius of alkali metal ions and all the anions except Ph_4B^- and Pi^- ions have been taken from Nightingale.[103] Ionic radii of tetraalkyl ammonium ions and Ph_4B^- are taken from Krumgalz,[104] and that of Pi^- has been taken from Gilkerson and Stamm.[105] For chemical names of the various ions, please see the figure caption.

In water, it is seen that the ionic conductivity is significantly larger for K^+, Rb^+, and Cs^+ with little difference between their values (1.33–1.69 Å). Also note that their ionic radii vary over a narrow range as compared to other ions. For anions in water, Cl^-, Br^-, and I^- have large conductivities as compared to other ions. Again their radii lie within a narrow range (1.81–2.16 Å). The value of conductivity has increased from around 39 to around 78 S cm^2 mol^{-1} on going from Li^+ to Rb^+. The increase in conductivity for the anion is around the same range. The observed conductivity–ionic radius plot for EG is similar to that for water with a maximum around the same ionic radius for both cations and anions. The change in the value of conductivity is, however, over a narrower range (2–5 S cm^2 mol^{-1}). For methanol, a similar increase in λ^0 followed by a decrease is seen, but the maximum in λ^0 is now seen for ions of larger size, in the case of both cations as well as anions. For cations, the maximum in λ^0 is seen for TMA^+. For anions, it is seen for ClO_4^-.

We now examine the observed λ^0–r_i behavior in terms of previous investigations on dependence of diffusion on ionic radius.[14,53,54] The ions diffuse through the void network of the solvent by migrating from one void to another. While doing so, the ion has to pass through the bottleneck which is the narrower part of the void network. We note that the void network is dynamically altered in time. Previous studies by Derouane and co-workers and our own[53,54,114,115] have shown that the ion whose diameter is comparable to the diameter of the neck has an easy passage since, in this case, the forces exerted on the solute by the host mutually cancel each other due to symmetry. The ion experiences lower net force which decreases the friction and therefore increases the ionic conductivity or diffusivity. Our own recent work of ions of differing sizes diffusing within liquid water has shown that a maximum in diffusivity is seen when the ionic radius is varied.[14,53,54,116] Further, it has been demonstrated that the ion with maximum diffusivity is associated with lower net force. Another distinguishing characteristic of this anomalous maximum in diffusivity is the lower activation energy.[117] The anomalous maximum in diffusivity is referred to as the Levitation effect. Anomalous maximum as a function of the size of the diffusant is observed in a wide variety of condensed matter phases and provides a unified explanation with the help of the dimensionless Levitation parameter (γ), which is defined as the ratio of the distance at which the interaction is optimum ($2^{1/6}\sigma_{iw}$) between the ion and the solvent to the radius of the bottleneck ($\sigma_n/2$):

$$\gamma = \frac{2^{1/6}\sigma_{iw}}{\sigma_n/2} \tag{8}$$

A maximum is seen when γ is close to unity for crystalline, well-ordered solids. For systems with disorder such as a liquid, the maximum is seen when γ is close to 0.6.[118] As shown in eq 8, the numerator of the expression is strongly influenced by the ion–solvent interaction, in particular, the solute diameter. The denominator is sensitive to the void structure which is determined by the solvent structure. Any change in density or pressure leads to variation in the void structure and solvent properties which in turn alters the denominator of the expression for γ. Thus, according to Levitation effect, the precise details in the size-dependence of ionic conductivity in any solvent will depend upon the void and neck distribution in the solvent.

In the previous subsection, we have seen that the void and neck distribution of both water and EG overlap considerably suggesting that the sizes of voids as well as necks existing within these two solvents are similar. This result, coupled with the discussion above implies that the dependence of λ^0 with r_i should be similar in these two solvents. Further, the ion with maximum conductivity should be around the same value of ionic radius, r_i. This is what is seen in Figure 11. The distribution of void and neck in the case of methanol, as we saw

dx.doi.org/10.1021/jp4036919 | J. Phys. Chem. B 2013, 117, 8196–8208

earlier, was shifted toward larger radius or sizes (see Figure 11). As the sizes of the necks in methanol solvent are larger, it is to be expected that the size of the solute at which the maximum in λ^0 will be seen in the plot of λ^0-r_i will also be larger and is given by:

$$\sigma_{iw} = \frac{(\sigma_n/2).\ \gamma}{2^{1/6}} \tag{9}$$

where γ is close to 0.6. The whole curve λ^0-r_i is shifted to larger radius since the void as well as neck distributions are similarly shifted to larger sizes. Thus, this explains the observed shift of λ^0-r_i leading to maximum for TMA^+ (2.80 Å) instead of Rb^+ (1.48 Å) observed for water and EG. The sign of the charge does not alter the arguments given by Levitation effect. Therefore we expect anions to behave similarly. For anions, we see that λ^0 is maximum for Cl^- ion (r_i = 1.81 Å) in water and EG. In methanol, the maximum shifts to ClO_4^- ion with radius 2.92 Å. Thus, r_i^{max} ion with maximum λ^0 is seen to be $r_i^{max}(water) \approx r_i^{max}(EG) \leq r_i^{max}(methanol)$.

Thus, from the void and neck distribution we are able to understand the reasons why the limiting ion conductivity is maximum for larger-sized ions in some of the solvents. The principal reason for shift of the maximum to larger-sized ion in methanol appears to be its low density which leads to larger-sized voids and necks within the liquid medium. These are consistent with our recent study on dependence of diffusivity on solute diameter and the role of density and disorder in Lennard-Jones system.[119]

Recently, Chandra and co-workers have reported the MD simulation studies on dependence of conductivity of as a function of ionic radius for various alkali metal cations, halide anions as well as tetraalkylammonium cations in methanol.[25] They observed a shift in the ionic radius at which the maximum in conductivity is seen to larger sizes of cation in methanol as compared to water. The shift is from from Rb^+ in water to TMA^+ in methanol. In case of anions, they observed monotonic increase in conductivity up to iodide ion.[25] However, our analysis of experimental results and arguments in terms of the Levitation effect, (see Figure 11) show that there should and indeed exists a maximum in conductivity. This is seen for a still larger sized anion, namely, for ClO_4^-.

Above analysis of experimental results suggests that not only is the solvent structure important but along with it, the void structure and the density plays an important role in deciding the trend in size dependence of ionic conductivity in different polar solvents.

A quantitative prediction of the size of the ion from the expression for the levitation parameter (see eq 8) is made difficult for the following reasons. The void and neck distributions have been obtained by assuming that the diameters of the solvent molecules are given by their respective van der Waals diameters. However, since the interactions between the solvent molecules includes electrostatic interactions, use of van der Waals diameters is an approximation and does not reflect the true dimensions of the void and neck. Further since definition of a radius in the presence of long-range interactions is not easy, we have to use the van der Waals radius in the Voronoi construction. For this reason the values to be used in the denominator for the expression of levitation parameter is imprecise.

A possible explanation on why there is deviation from SE relation (see eq 1) in the plot of diffusivity against reciprocal viscosity is discussed here. We attribute the higher diffusivity of lithium and chloride ions in water seen in Figures 3 and 4 to the enhanced diffusivity due to the influence of the ionic radius on diffusivity discussed above. We have seen from Figure 11 that both lithium and chloride ions lie in the anomalous regime of the Levitation effect for water and EG. As a result their diffusivities are enhanced over and above predicted by SE relation. However, only conducitivity of these ions in water exhibits a deviation from $D-1/\eta$ dependence and not EG. This could probably because the enhancement in diffusivity of these ions in water is much more significant as compared to EG. More studies are required to test the validity of this explanation.

4. CONCLUSIONS

We have investigated the solvation structure, self-diffusion coefficient (D) and mean residence time (MRT) for LiCl in water, methanol, and ethylene glycol (EG) using molecular dynamics simulation at 298 K.

The study suggests that the reciprocal relation between the self-diffusivity or limiting ion conductivity of a solute and the viscosity of the solution indeed is valid with certain exceptions. We believe these exceptions arise when the ion has a radius which lies in the anomalous regime of the Levitation effect. It is seen that in water and methanol, ion−solvent interactions are stronger than the solvent−solvent interactions. In EG, ion−solvent and solvent−solvent interactions are comparable.

It is also seen that apart from the solvent structure, the density has a strong influence on the radius of the void and necks within these liquids. It is shown that the distribution of voids and necks can help us to understand the variation of limiting ionic conductivity with ionic radius. More specifically, it can tell us why the limiting ionic conductivity is maximum for ions of larger size in solvents such as methanol. We have shown that this is related to the larger voids and necks present in methanol. The maximum in the plot of λ^0 versus r_i shifts to larger sizes for both cations and anions. This is the prediction of the Levitation effect. It may, however, stressed here that all existing Voronoi constructions techniques assume the atoms or molecules to be spherical objects. Approximating molecules as spheres may not always be a valid and might lead to inaccurate estimates for the void and neck diameters.

The present study suggests that the magnitude of the limiting ion conductivity λ^0 is determined by the viscosity. In contrast, the variation of λ^0 as a function of ionic radius is a function of the void and neck distribution. It is important to note that two different properties of the solvent determine the final Stokes−Einstein−Walden relation between self-diffusivity, viscosity, and ionic radius.

AUTHOR INFORMATION

Corresponding Author

*E-mail: yashonat@sscu.iisc.ernet.in.

Notes

The authors declare no competing financial interest.

ACKNOWLEDGMENTS

Authors thank Department of Science and Technology, New Delhi for a nano mission TUE project and Ramanna Fellowship to S.Y. and financial support under Fast Track scheme to P.K. Authors also thank CSIR, New Delhi for financial support through a grant.

REFERENCES

(1) Enderby, J. E.; Neilson, G. W. *The Physics and Physical Chemistry of Water*; Franks, F., Eds.; Plenum Press: New York, 1972; Vol. *1*.

(2) Gores, H. J.; Barthel, J. Nonaqueous Electrolyte Solutions: New Materials for Devices and Processes Based on Recent Applied Research. *Pure Appl. Chem.* **1995**, *67*, 919−930.

(3) Ohtaki, H.; Radnai, T. Structure and Dynamics of Hydrated Ions. *Chem. Rev.* **1993**, *93*, 1157−1204.

(4) Omta, A. W.; Kropman, M. F.; Woutersen, S.; Bakker, H. J. Negligible Effect of Ions on the Hydrogen-Bond Structure in Liquid Water. *Science* **2003**, *301*, 347−349.

(5) Mancinelli, R.; Botti, A.; Bruni, F.; Ricci, M. A.; Soper, A. K. Perturbation of Water Structure due to Monovalent Ions in Solution. *Phys. Chem. Chem. Phys.* **2007**, *9*, 2959−2967.

(6) Mancinelli, R.; Botti, A.; Bruni, F.; Ricci, M. A.; Soper, A. K. Hydration of Sodium, Potassium, and Chloride Ions in Solution and the Concept of Structure Maker/Breaker. *J. Phys. Chem. B* **2007**, *111*, 13570−13577.

(7) Marcus, Y. Effect of Ions on the Structure of Water: Structure Making and Breaking. *Chem. Rev.* **2009**, *109*, 1346−1370.

(8) Tielrooij, K. J.; Garcia-Araez, N.; Bonn, M.; Bakker, H. J. Cooperativity in Ion Hydration. *Science* **2010**, *328*, 1006−1009.

(9) Laage, D.; Stirnemann, G.; sterpone, F.; Rey, R.; Hynes, J. T. Reorientation and Allied Dynamics in Water and Aqueous Solutions. *Annu. Rev. Phys. Chem.* **2011**, *62*, 395−416.

(10) Ohtaki, H. Ionic Solvation in Aqueous and Nonaqueous Solutions. *Monatsh. Chem.* **2001**, *132*, 1237−1268.

(11) Spangberg, D.; Hermanson, K. Effective Three-body Potentials for Li^+(aq) and Mg^{2+}(aq). *J. Chem. Phys.* **2003**, *119*, 7263−7281.

(12) Egorov, A. V.; Komolkin, A. V.; Chizhik, V. I.; Yushmanov, P. V.; Lyubartsev, A. P.; Laaksonen, A. Temperature and Concentration Effects on Li^+-Ion Hydration. A Molecular Dynamics Simulation Study. *J. Phys. Chem. B* **2003**, *107*, 3234−3242.

(13) Bagchi, B.; Biswas, R. Ionic Mobility and Ultrafast Solvation: Control of a Slow Phenomenon by Fast Dynamics. *Acc. Chem. Res.* **1998**, *31*, 181−187.

(14) Ghorai, P. K.; Yashonath, S.; Lynden-Bell, R. M. Size-Dependent Maximum in Ion Conductivity: The Levitation Effect Provides an Alternative Explanation. *J. Phy. Chem. B* **2005**, *109*, 8120−8124.

(15) Rasaiah, J. C.; Lynden-Bell, R. M. Computer Simulation Studies of the Structure and Dynamics of Ions and Non-polar Solutes in Water. *Phil. Trans. R. Soc., London A* **2001**, *359*, 1545−1574.

(16) Walser, R.; Mark, A. E.; Gunsteren, W. F. V. On the Validity of Stoke's Law at the Molecular Level. *Chem. Phys. Lett.* **1999**, *303*, 583−586.

(17) Alder, B. J.; Gass, M.; Wainwright, T. E. Studies in Molecular Dynamics. VIII. The Transport Coefficients for a Hard-Sphere Fluid. *J. Chem. Phys.* **1970**, *53*, 3813−3826.

(18) Berner, B.; Kivelson, D. Paramagneticallly Enhanced Relaxation of Nuclear Spins. Measurement of Diffusion. *J. Phys. Chem.* **1979**, *83*, 1401−1405.

(19) Lamanna, R.; Delmelle, M.; Cannistraro, S. Solvent Stokes-Einstein Violation in Aqueous Protein Solutions. *Phys. Rev. E* **1994**, *49*, 5878−5880.

(20) Willeke, M. Limits of the Validity of the Mass Ratio Independence of the Stokes-Einstein Relation: Molecular Dynamics Calculations and Comparison with the Enskog Theory. *Mol. Phys.* **2003**, *101*, 1123−1130.

(21) Berendsen, H. J. C.; Grigera, J. R.; Straatsma, T. P. The Missing Term in Effective Pair Potentials. *J. Phys. Chem.* **1987**, *91*, 6269−6271.

(22) Haughney, M.; Ferrario, M.; McDonald, I. R. Pair Interactions and Hydrogen-bond Networks in Models of Liquid Methanol. *Mol. Phys.* **1986**, *58*, 849−853.

(23) Haughney, M.; Ferrario, M.; McDonald, I. R. Molecular-Dynamics Simulation of Liquid Methanol. *J. Phys. Chem.* **1987**, *91*, 4934−4940.

(24) Chowdhury, S.; Chandra, A. Hydration Structure and Diffusion of Ions in Supercooled Water: Ion Size Effects. *J. Chem. Phys.* **2003**, *118*, 9719−9725.

(25) Chowdhuri, S.; Chandra, A. Solute Size Effects on the Solvation Structure and Diffusion of Ions in Liquid Methanol under Normal and Cold Conditions. *J. Chem. Phys.* **2006**, *124*, 084507−1−084507−8.

(26) Chopra, D.; Row, T. N. G.; Arunan, E.; Klein, R. A. Crystalline Ethane-1,2-diol does not have Intra-molecular Hydrogen Bonding: Experimental and Theoretical Charge Density Studies. *J. Mol. Struct.* **2010**, *964*, 126−133.

(27) Jorgensen, W. L.; Maxwell, D. S.; Tirado-Rives, J. Development and Testing of the OPLS All-Atom Force Field on Conformational Energetics and Properties of Organic Liquids. *J. Am. Chem. Soc.* **1996**, *118*, 11225−11236.

(28) Szefczyk, B.; Cordeiro, M. N. D. S. Physical Properties at the Base for the Development of an All-Atom Force Field for Ethylene Glycol. *J. Phys. Chem. B* **2011**, *115*, 3013−3019.

(29) Fennell, C. J.; Bizjak, A.; Vlachy, V.; Dill, K. A. Ion Pairing in Molecular Simulations of Aqueous Alkali Halide Solutions. *J. Phys. Chem. B* **2009**, *113*, 6782−6791.

(30) Forester, T. R.; Smith, W. *The DL-POLY-2.0 Reference Manual*, version 2.0; CCLRC, Daresbury Laboratory: Warrington, U.K., 1985.

(31) Allen, M. P.; Tildesley, D. J. *Computer Simulation of Liquids*; Clarendon Press: Oxford, 1987.

(32) Corti, D. S.; Debenedetti, P. G.; Sastry, S.; Stillinger, F. H. Constraints, Metastability, and Inherent Structures in Liquids. *Phys. Rev. E* **1997**, *55*, 5522−5534.

(33) Sastry, S.; Corti, D. S.; Debenedetti, P. G.; Stillinger, F. H. Statistical Geometry of Particle Packings. I. Algorithm for Exact Determination of Connectivity, Volume, and Surface Areas of Void Space in Monodisperse and Polydisperse Sphere Packings. *Phys. Rev. E* **1997**, *56*, 5524−5532.

(34) Weissberg, H. L.; Prager, S. Viscous Flow through Porous Media. II. Approximate ThreePoint Correlation Function. *Phys. Fluid* **1962**, *5*, 1390−1392.

(35) Shahinpoor, M. Statistical Mechanical Considerations on the Random Packing of Granular-Materials. *Powder Technol.* **1980**, *25*, 163−176.

(36) Ghorai, P. K.; Yashonath, S. The Stokes-Einstein Relationship and the Levitation Effect: Size-Dependent Diffusion Maximum in Dense Fluids and Close-Packed Disordered Solids. *J. Phy. Chem. B* **2005**, *109*, 5824−5835.

(37) Tanemura, M.; Ogawa, T.; Ogita, N. A New Algorithm for Three-dimensional Voronoi Tessellation. *J. Comput. Phys.* **1983**, *51*, 191−207.

(38) Gellatly, B.; Finney, J. Characterisation of models of multicomponent amorphous metals: The radical alternative to the Voronoi polyhedron. *J. Non-Cryst. Solids* **1982**, *50*, 313−329.

(39) Alinchenko, M.; Anikeenko, A.; Medvedev, N.; Voloshin, V.; Mezei, M.; Jedlovszky, P. Morphology of Voids in Molecular Systems. A Voronoi-Delaunay Analysis of a Simulated DMPC Membrane. *J. Phys. Chem. B* **2004**, *108*, 19056−19067.

(40) Mezei, M. Modified proximity criteria for the analysis of the solvation of a polyfunctional solute. *Mol. Simul.* **1988**, *1*, 327−332.

(41) Bowen, T. C.; Li, S.; Noble, R. D.; Falconer, J. L. Driving Force for Pervaporation Through Zeolite Membranes. *J. Membr. Sci.* **2003**, *225*, 165−176.

(42) ten Elshof, J. E.; Abadal, C. R.; Sekulic, J.; Chowdhury, S. R.; Blank, D. H. A. Transport Mechanisms of Water and Organic Solvents Through Microporous Silica in the Pervaporation of Binary Liquids. *Microporous Mesoporous Mater.* **2003**, *65*, 197−208.

(43) Hu, C.; Guo, R.; Li, B.; Ma, X.; Wu, H.; Jiang, Z. Development of Novel Mordenite-filled Chitosan-poly(acrylic acid) Polyelectrolyte Complex Membranes for Pervaporation Dehydration of Ethylene Glycol Aqueous Solution. *J. Membr. Sci.* **2007**, *293*, 142−150.

(44) Ueno, M.; Tsuchihashi, N.; Yoshida, K.; Ibuki, K. Pressure and Solvent Isotope Effects on the Mobility of Monovalent Cations in Water. *J. Chem. Phys.* **1996**, *105*, 3662−3670.

(45) Kay, R. L.; Vituccio, T.; Zawoyski, C.; Evans, D. F. Viscosity B Coefficients for Tetraalkylammonium Halides. *J. Phys. Chem.* **1966**, *70*, 2336−2341.
(46) Kalugin, O. N.; Lebed, A. V.; Vyunnik, I. N. Properties of 1−1 Electrolytes Solutions in Ethylene Glycol at Temperatures from 5 to 175 °C: Part 2 Limiting Ion Conductances and Ion-molecule Interactions. *J. Chem. Soc. Faraday Trans.* **1998**, *94*, 2103−2107.
(47) Rauf, M. A.; Stewart, G. H. Farhataziz, Viscosities and Densities of Binary-mixtures of 1-Alkanols from 15 °C to 55 °C. *J. Chem. Eng. Data* **1983**, *28*, 324−328.
(48) Dean, J. A. *Langès Handbook of Chemistry*, 15th ed.; McGraw-Hill Book Co.: New York, 1999; p 5.115.
(49) Chumaevskii, N. A.; Rodnikova, M. N.; Barthel, J. Some Peculiarities of Compounds with Spatial H-bond Network: H_2O, H_2O_2, $HOCH_2CH_2OH$. *J. Mol. Liq.* **2004**, *115*, 63−67.
(50) Zhao, Y.; Freeman, G. R. Solvent Effects on the Reactivity of Solvated Electrons with NO_3,S- in C-1 to C-4 Alcohols. *Can. J. Chem.* **1995**, *73*, 284−288.
(51) DeSieno, R. P.; Greco, P. W.; Mamajek, R. C. The Conductance of Tetraalkylammonium Halides in Ethylene Glycol. *J. Phys. Chem.* **1971**, *75*, 1722−1726.
(52) Robinson, R. A.; Stokes, R. H. *Electrolyte Solutions*, 2nd revised ed.; Dover Publications, New York, 2002.
(53) Ghorai, P. K.; Yashonath, S. Existence of a Size-Dependent Diffusivity Maximum for Uncharged Solutes in Water and its Implications. *J. Phy. Chem. B* **2006**, *110*, 12072−12079.
(54) Ghorai, P. K.; Yashonath, S. Evidence in Support of Levitation Effect as the Reason for Size Dependence of Ionic Conductivity in Water: A Molecular Dynamics Simulation. *J. Phy. Chem. B* **2006**, *110*, 12179−12190.
(55) Krumgalz, B. Separation of Limiting Equivalent Conductances into Ionic Contributions in Non-Aqueous Solutions by Indirect Methods. *J. Chem. Soc. Faraday Trans. 1* **1983**, *79*, 571−587.
(56) Safonova, L. P.; Patsatsiya, B. K.; Kolker, A. M. Electro-conductivity of Individual Ions and their Association in Acetonitrile at 233−318K. *Zh. Fiz. Khim.* **1992**, *66*, 2201−2208.
(57) Carrion, G. G.; Vrabec, J.; Hasse, H. Prediction of Self-diffusion Coefficient and Shear Viscosity of Water and its Binary Mixtures with Methanol and Ethanol by Molecular Simulation. *J. Chem. Phys.* **2011**, *134*, 74508−1−74508−14.
(58) Mark, P.; Nilsson, L. Structure and Dynamics of the TIP3P, SPC, and SPC/E Water Models at 298 K. *J. Phys. Chem. A* **2001**, *105*, 9954−9960.
(59) Guardia, E.; Sese, G.; Padro, J. On The Hydrogen-Bonding Effects in Liquid Methanol - A Molecular Dynamics Simulation Study. *J. Mol. Liq.* **1994**, *62*, 1−16.
(60) Saiz, L.; Padro, J. A.; Guardia, E. Structure of Liquid Ethylene Glycol: A Molecular Dynamics Simulation Study with Different Force Fields. *J. Chem. Phys.* **2001**, *114*, 3187−3199.
(61) Price, W. S.; Ide, H.; Arata, Y. Self-Diffusion of Supercooled Water to 238 K Using PGSE NMR Diffusion Measurements. *J. Phys. Chem. A* **1999**, *103*, 448−450.
(62) Hurle, R. L.; Woolf, L. A. The Effect of Isotopic-Substitution on Self-Diffusion in Methanol Under Pressure. *Aut. J. Chem.* **1980**, *33*, 1947−1952.
(63) Chandrasekhar, N.; Krebs, P. The Spectra and the Relative Yield of Solvated Electrons Produced by Resonant Photodetachment of Iodide Anion in Ethylene Glycol in the Temperature Range $296 \leq T \leq 453$K. *J. Chem. Phys.* **2000**, *112*, 5910−5914.
(64) Koneshan, S.; Rasaiah, J. C.; Lynden-Bell, R. M.; Lee, S. H. Solvent Structure, Dynamics, and Ion Mobility in Aqueous Solutions at 25 °C. *J. Phys. Chem. B* **1998**, *102*, 4193−4204.
(65) Head-Gordon, T.; Hura, G. Water Structure from Scattering Experiments and Simulation. *Chem. Rev.* **2002**, *102*, 2651−2670.
(66) Svishchev, I. M.; Kusalik, P. G. Structure in Liquid Methanol from Spatial Distribution Functions. *J. Chem. Phys.* **1994**, *100*, 5165−5171.
(67) D'Angelo, P.; Nola, A. D.; Mangoni, M.; Pavel, N. V. An Extended X-ray Absorption Fine Structure Study by Employing Molecular Dynamics Simulations: Bromide Ion in Methanolic Solution. *J. Chem. Phys.* **1996**, *104*, 1779−1790.
(68) Kosztolanyi, T.; Bako, I.; Palinkas, G. Hydrogen Bonding in Liquid Methanol, Methylamine, and Methanethiol Studied by Molecular-Dynamics Simulations. *J. Chem. Phys.* **2003**, *118*, 4546−4555.
(69) Jorgensen, W. L. Optimized Intermolecular Potential Functions for Liquid Alcohols. *J. Phys. Chem.* **1986**, *90*, 1276−1284.
(70) Sarkar, S.; Joarder, R. N. Molecular Clusters and Correlations in Liquid Methanol at Room Temperature. *J. Chem. Phys.* **1993**, *99*, 2032−2039.
(71) Soper, A. K.; Bruni, F.; Ricci, M. A. Site-site Pair Correlation Functions of Water from 25 to 400 °C: Revised Analysis of New and Old Diffraction Data. *J. Chem. Phys.* **1997**, *106*, 247−254.
(72) Spangberg, D.; Rey, R.; Hynes, J. T.; Hermansson, K. Rate and Mechanisms for Water Exchange Around Li^+(aq) from MD Simulations. *J. Phys. Chem. B* **2003**, *107*, 4470−4477.
(73) Impey, R. W.; Sprik, M.; Klein, M. L. Ionic Solvation in Nonaqueous Solvents - The Structure of Li^+ and Cl^- in Methanol, Ammonia, and Methylamine. *J. Am. Chem. Soc.* **1987**, *109*, 5900−5904.
(74) Pagliai, M.; Cardini, G.; Schettino, V. Solvation Dynamics of Li^+ and Cl^- Ions in Liquid Methanol. *J. Phys. Chem. B* **2005**, *109*, 7475−7481.
(75) Megyes, T.; Radnai, T.; Grosz, T.; Palinkas, G. X-ray Diffraction Study of Lithium Halides in Methanol. *J. Mol. Liq.* **2002**, *101*, 3−18.
(76) Chandrasekhar, J.; Spellmeyer, D. C.; Jorgensen, W. L. Energy Component Analysis for Dilute Aqueous-Solutions of Li^+, Na^+, F^-, and Cl^- Ions. *J. Am. Chem. Soc.* **1984**, *106*, 903−910.
(77) Heinzinger, K. Computer Simulations of Aqueous Electrolyte Solutions. *Phys. B C* **1985**, *131*, 196−216.
(78) Mezei, M.; Beveridge, D. Monte Carlo Studies of the Structure of Dilute Aqueous Solutions of Li^+, Na^+, K^+, F^-, and Cl^-. *J. Chem. Phys.* **1981**, *74*, 6902−6910.
(79) Duan, Z.; Zhangi, Z. Solvation Properties of Li^+ and Cl^- in Water: Molecular Dynamics Simulation with a Non-rigid Model. *Mol. Phys.* **2003**, *101*, 1501−1510.
(80) Enderby, J. E.; Neilson, G. W. *Water: A Comprehensive Treatise*; Franks, F., Ed.; New York: Plenum, 1979; Vol. *6*
(81) Cummings, S.; Enderby, J. E.; Neilson, G. W.; Newson, J. R.; Howe, R. A.; Howells, W. S.; Soper, A. K. Chloride-Ions in Aqueous Solutions. *Nature* **1980**, *287*, 714−716.
(82) Sese, G.; Guardia, E.; Padro, J. A. Molecular Dynamics Study of Na^+ and Cl^- in Methanol. *J. Chem. Phys.* **1996**, *105*, 8826−8834.
(83) Impey, R. W.; Madden, P. A.; McDonald, I. R. Hydration and Mobility of Ions in Solution. *J. Phys. Chem.* **1983**, *87*, 5071−5083.
(84) Northrup, S. H.; Hynes, J. T. The Stable States Picture of Chemical Reactions. I. Formulation for Rate Constants and Initial Condition Effects. *J. Chem. Phys.* **1980**, *73*, 2700−2714.
(85) Laage, D.; Hynes, J. T. On the Residence Time for Water in a Solute Hydration Shell: Application to Aqueous Halide Solutions. *J. Phys. Chem. B* **2008**, *112*, 7697−7701.
(86) Furth, R. I. The Statistical Treatment of the Thermodynamics of Liquids by the Theory of Holes. *Proc. Cambr. Philos. Soc.* **1941**, *37*, 252−275.
(87) Furth, R. On the Theory of the Liquid State III. The Hole Theory of the Viscous Flow of Liquids. *Proc. Cambr. Philos. Soc.* **1941**, *37*, 281−290.
(88) Hunter, C. A. A Surface Site Interaction Model for the Properties of Liquids at Equilibrium. *Chem. Sci.* **2013**, *4*, 1687−1700.
(89) Ohmine, I.; Tanaka, H. Fluctuation, Relaxations, and Hydration in Liquid Water-Hydrogen-Bond Rearrangement Dynamics. *Chem. Rev.* **1993**, *93*, 2545−2566.
(90) Bellisent-Funel, M. C., Dore, J. C., Eds.; *Hydrogen-Bond Networks*; Kluwer: Dordrecht, 1994.
(91) Ladanyi, B. M.; Skaf, M. S. Computer-Simulation of Hydrogen-Bonding Liquids. *Annu. Rev. Phys. Chem.* **1993**, *44*, 335−368.
(92) Padro, J. A.; Saiz, L.; Guardia, E. Hydrogen Bonding in Liquid Alcohols: A Computer Simulation Study. *J. Mol. Struct.* **1997**, *416*, 243−248.

(93) Bako, J.; Grosz, T.; Palinkas, G.; Bellissent-Funel, M. C. Ethylene Glycol Dimers in the Liquid Phase: A Study by X-ray and Neutron Diffraction. *J. Chem. Phys.* **2003**, *118*, 3215−3221.
(94) Gubskaya, A. V.; Kusalik, P. G. Molecular Dynamics Simulation Study of Ethylene Glycol, Ethylenediamine, and 2-Aminoethanol. 1. The Local Structure in Pure Liquids. *J. Phy. Chem. A* **2004**, *108*, 7151−7164.
(95) Rodnikova, M. N.; Chumaevskii, N. A.; Troitskii, V. M.; Kayumora, D. B. Structure of Liquid Ethylene Glycol. *Russ. J. Phys. Chem.* **2006**, *80*, 826−830.
(96) Rodnikova, M.; Barthel, J. Elasticity of the Spatial Network of Hydrogen Bonds in Liquids and Solutions. *J. Mol. Liq.* **2007**, *131−132*, 121−123.
(97) de Oliveira, O. V.; Freitas, L. C. G. Molecular Dynamics Simulation of Liquid Ethylene Glycol and its Aqueous Solution. *J. Mol. Struct. (THEOCHEM)* **2005**, *728*, 179−187.
(98) Tanaka, H. Cavity Distribution in Liquid Water and Hydrophobic Hydration. *Chem. Phys. Lett.* **1998**, *282*, 133−138.
(99) Graziano, G. Water: Cavity Size Distribution and Hydrogen Bonds. *Chem. Phys. Lett.* **2004**, *396*, 226−231.
(100) in't Veld, P. J.; Stone, M. J.; Truskett, T. M.; Sanchez, I. C. Liquid Structure via Cavity Size Distributions. *J. Phys. Chem. B* **2000**, *104*, 12028−12034.
(101) Voronoi, G. Nouvelles Applications Des Parametres Continus a la Theorie Des Formes Quadratiques. *J. Reine Angew. Math* **1908**, *134*, 198−287.
(102) Azaroff, L. V. *Solid State Physics*; McGraw-Hill Book Co.: New York, 1960.
(103) Nightingale, E. R. Phenomenological Theory of Ion Solvation. Effective Radii of Hydrated Ions. *J. Phys. Chem.* **1959**, *63*, 1381−1387.
(104) Krumgalz, B. S. Dimensions of Tetra-alkyl(ary1)onium Ions. *J. Chem. Soc., Faraday Trans. 1* **1982**, *78*, 437−449.
(105) Gilkerson, W. R.; Stamm, R. E. The Conductance of Tetra-Normal-Butylammonium Picrate in Benzene-Ortho-Dichlorobenzene Solvent Mixtures at 25-Degrees. *J. Am. Chem. Soc.* **1960**, *82*, 5295−5298.
(106) Nakahara, M.; Zenke, M.; Ueno, M.; Shimizu, K. Solvent Isotope Effect on Ion Mobility in Water at High Pressure. Conductance and Transference Number of Potassium Chloride in Compressed Heavy Water. *J. Chem. Phys.* **1985**, *83*, 280−287.
(107) Hefter, G. T.; Salomon, M. Conductivities of KF and CsF in Methanol at 25 °C. *J. Sol. Chem.* **1996**, *25*, 541−553.
(108) Kay, R. L.; Evans, D. F. The Effect of Solvent Structure on the Mobility of Symmetrical Ions in Aqueous Solution. *J. Phys. Chem.* **1966**, *70*, 2325−2335.
(109) Santos, M. C.; Spiro, M. Transference Numbers of Potassium Chloride and Ionic Conductances in Ethylene Glycol at 25 °C. *J. Phys. Chem.* **1972**, *76*, 712−720.
(110) Broadwater, T. L.; Kay, R. L. The Temperature Coefficient of Conductance for the Alkali Metal, Halide, Tetraalkylammonium,Halide, Halate, and Perhalate Ions in D_2O. *J. Sol. Chem.* **1975**, *4*, 745−762.
(111) Majeed, N. N.; Timimi, B. A. Conductance of n-Alkylammonium and n-Alkanolammonium Chlorides and Picrates in Water at 25 °C. *J. Sol. Chem.* **1981**, *10* (4), 253−262.
(112) Evers, E. C.; Knox, A. G. Conductivity Studies in Methanol. *J. Am. Chem. Soc.* **1951**, *73*, 1739−1744.
(113) Kunze, R. W.; Fuoss, R. M. Conductance of the Tetraphenylboride Ion in Methanol. *J. Phys. Chem.* **1963**, *67*, 385−386.
(114) Derouane, E. G. The Energetics of Sorption by Molecular-Sieves - Surface Curvature Effects. *Chem. Phys. Lett.* **1987**, *142*, 200−204.
(115) Derouane, E. G.; Andre, J. M.; Lucas, A. Surface Curvature Effects in Physisorption and Catalysis by Microporous Solids and Molecular Sieves. *J. Catal.* **1988**, *110*, 58−73.
(116) Yashonath, S.; Ghorai, P. K. Diffusion in Nanoporous Phases: Size Dependence and Levitation Effect. *J. Phys. Chem. B* **2008**, *112*, 665−686.
(117) Yashonath, S.; Santikary, P. Diffusion of Sorbates in Zeolites Y and A Novel Dependence on Sorbate Size and Strength of Sorbate-Zeolite Interaction. *J. Phys. Chem.* **1994**, *98*, 6368−6376.
(118) Ghorai, P. K.; Kumar, A. V. A.; Sastry, S.; Yashonath, S. Diffusion Maximum as a Function of Size in Dense Liquids. *Phy. Rev. E* **2005**, *72*, 030202(R)-1−030202(R)-4.
(119) Varanasi, S. R.; Kumar, P.; Yashonath, S. Dependence of Diffusivity on Density and Solute Diameter in Liquid Phase: A Molecular Dynamics Study of Lennard-Jones System. *J. Chem. Phys.* **2012**, *136*, 144505−1−144505−11.